

ANALYSIS OF THERMOCOUPLE BEHAVIOR IN COMPARTMENT FIRES

S.C. Kim, A. Hamins, M.F. Bundy, G.H. Ko and E.L. Johnsson
National Institute of Standards and Technology, Gaithersburg, MD 20899-8663 USA

ABSTRACT

To examine the uncertainty of thermocouple temperature measurements, the present study uses numerical simulations and analytical solutions to investigate the heat transfer processes associated with bare bead and double shield aspirated thermocouple. This study is divided into two parts. First, three dimensional CFD (Computational Fluid Dynamics) calculations for real geometry are performed to understand the flow characteristics of the double shielded aspirated thermocouple. Based on isothermal flow calculations for real geometry, conjugate heat transfer calculations for a 3D simplified geometry are performed to investigate the thermocouple measurement error that may be important in a fire environment. The results of the 3D heat transfer calculation are compared with algebraic solutions from a previously developed simple energy balance model. The results predicted by the algebraic model were in agreement with the CFD model over a broad temperature range despite its many assumptions and idealizations. A parametric study was conducted to quantify the thermocouple errors for various gas temperature and surrounding conditions. The transient CFD solution provides information about the time response of the thermocouple measurement. In this manner, the present study improves our understanding of the uncertainty of thermocouple temperature measurements.

KEYWORDS: Thermocouple error, Aspirated thermocouple, Measurement uncertainty, CFD model

INTRODUCTION

Accurate measurement of the thermal field is one of the most basic ways to characterize a fire environment. Among the various techniques that can be used to measure the local temperature, bare bead thermocouples with a welded junction are probably the most common, and possibly the easiest to implement. Bare bead thermocouples have been widely used in numerous types of applications for many reasons, including their low cost, convenience, wide temperature range, suitability for large scale tests, robustness, and so on. In this sense, bare bead thermocouples are an indispensable part of fire research. On the other hand, the uncertainty associated with these measurements may be quite large, depending on the exact application or scenario and the measured temperature may be quite different from the actual gas temperature.

When a bare bead thermocouple is directly exposed to a fire environment, measurement error may result for a variety of reasons, such as radiative exchange between the bead junction and the surrounding environment, heat conduction along the thermocouple wire, soot deposition, thermal inertia, and catalytic effects. In order to reduce the measurement error of a bare bead thermocouple due to radiative exchange, the aspirated thermocouples is increasingly used in fire research applications. An aspirated thermocouple is a thermocouple which is shielded from the environment by a cylindrical tube. A gas sample from the location of interest is pulled into the aspiration tube, flowing past the thermocouple.^{1,2} Aspirated thermocouples can have a single or double shield configuration. In either case, the measurement error depends on the details of the environmental and operating conditions.

Recently, several studies have investigated the uncertainty of temperature measurement using bare bead and aspirated thermocouples. Newman et al.³ evaluated the effectiveness of bare bead and single shield aspirated thermocouples using data from a series of laboratory and room fire experiments. The simple steady heat-balance equations for aspirated thermocouples were utilized to determine the asymptotic value and compared with the measured results. Brohez et al.⁴ used two bare bead thermocouples to estimate radiation error in compartment fires, and a simple practical rule was

proposed to estimate the gas temperature using thermocouples with different bead diameters. The simple practical rule was validated with experiments and provided a rough estimate of the measurement bias associated with radiative exchange. Blevins and Pitts⁵ developed a steady-state algebraic energy balance model to characterize the bias associated with bare bead, single and double shielded aspirated thermocouple measurements. The effect of the aspiration velocity on the measurement uncertainty was investigated as a function of the conditions in a compartment fire. The simplified energy balance model has provided useful information about thermocouple measurement bias, but its accuracy is unclear, due to its many assumptions and approximations. The analytic model does not consider transient effects, local fluid flow, conductive heat transfer, or important details of the geometric configuration.

A detailed numerical approach is described in this study, which allows estimation of measurement uncertainty, with consideration of realistic boundary conditions. The numerical results are used to verify results from the simple energy balance model. The present study performed a series of CFD calculations to evaluate the measurement bias and response time, focusing on double shielded and bare bead thermocouples. The 3D CFD results are compared with algebraic solutions of a simplified energy balance model. The thermocouple uncertainty is characterized with the indicated thermocouple temperature and surrounding temperature. The transient CFD solution provides information about the time response of the thermocouple measurement and the time required to experimentally reach steady state.

NUMERICAL SIMULATION

A double shielded aspirated thermocouple is rather complicated, geometrically and operationally, whereas a bare bead thermocouple is relatively simple. The prototype aspirated thermocouple investigated in this study is double shielded with an end-hole adapted from NACA⁶ (National Advisory Committee for Aeronautics). Fig. 1 shows a schematic drawing of the probe with a close-up view of the inner cylinder and additional equipment. The geometrical complexity and aspiration flow causes a complicated flow field inside of this thermocouple. CFD is used to understand the detailed flow characteristics for this geometry, and to provide appropriate boundary conditions for a simplified analytic heat transfer model.

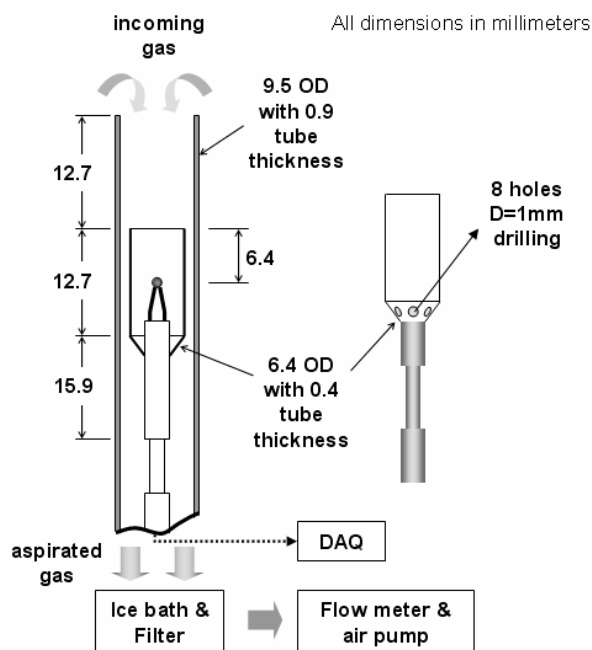


FIGURE 1. Schematic of the double shield aspirated thermocouple used in the NACA design⁶

A series of 3D CFD calculations have been performed to characterize the thermocouple bias for various conditions, representative of a compartment fire. Ideally, the CFD simulation would consider details of the flow and heat transfer in the actual geometry, including turbulence and conjugate heat transfer, but this would require prohibitively expensive computations. For this reason, the CFD calculations were split into two types. The first emphasized detailed calculations of the flow field for a real geometry, while the second involved detailed conjugate heat transfer calculations for a simplified geometry. The first considered the realistic geometry in order to understand details of the flow field associated with the double shield aspirated thermocouple. The second considered a simplified 3D geometry, focusing on details of the heat transfer process and with consideration for conduction, convection and radiation. Also, algebraic solutions of the previously developed simplified energy balance model ⁵ were obtained to compare with the 3D CFD results.

CFD Modeling of a Double Shield Aspirated Thermocouple

The flow fields are calculated using the commercially available CFD package FLUENT 6.0 ⁶ to model the flow for given operating conditions. The code is based on the finite volume method on a collocated grids, a non-staggered grid system is used for the storage of discrete velocities and pressures. The standard k-ε turbulence model and incompressible idealize gas assumption were applied to solve the Reynolds stress term and density change, respectively. The governing equation is discretized by the 2nd order upwind scheme in space and the SIMPLE (Semi-Implicit Method for Pressure Linked Equation) algorithm with under-relaxation is used to iteratively solve the momentum equation in their discretized form.

For the 3D flow calculation for the real geometry of a double shield aspirated thermocouple, the computational model includes an inner shield, an outer shield, a thermocouple bead and extended domain of the aspirated thermocouple. The computational domain including inside and outside of the double shield aspirated thermocouple is divided into approximately two million cells of tetrahedral type mesh using the ICFM-CFD which is the commercial CAD and grid generation program. Fig. 2 shows the computational grids of the double shield aspirated thermocouple.

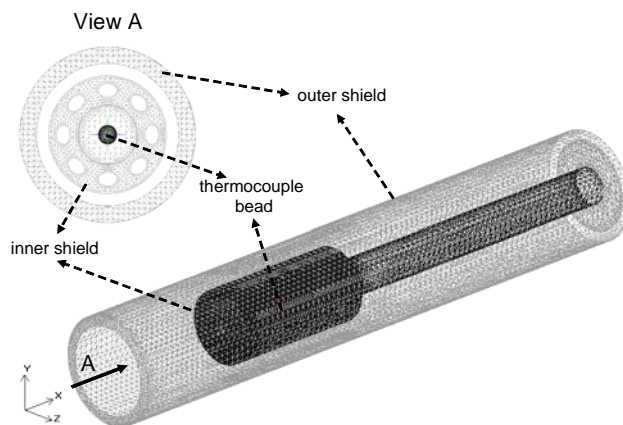


FIGURE 2. Computational grid used to model the end-open double shield aspirated thermocouple

Heat Transfer Modeling for a Simplified Geometry

Three dimensional heat transfer calculations that included conduction, convection and radiation were performed to estimate the measurement error for a bare bead and a double shield aspirated thermocouple for idealized simplified geometries. Fig. 3 shows a schematic of the idealized double shield aspirated thermocouple geometry considered here. The double shield thermocouple calculation assumed that the flow domain consisted of three flows: a flow about the outermost shield, an annular

flow between the outer and inner shields, and an inner flow within the inner shield. For the bare bead thermocouple calculation, the thermocouple bead was directly exposed to the local environment and the surroundings without shields or aspiration.

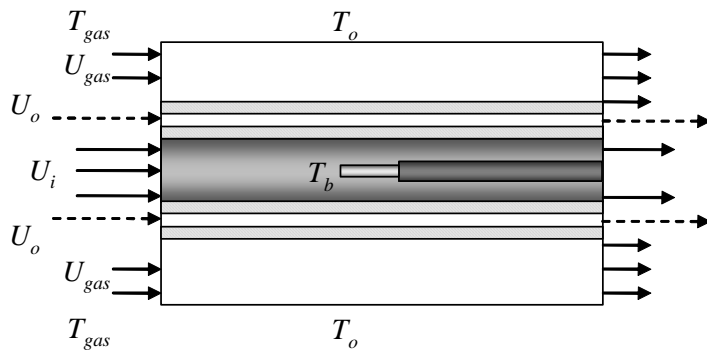


FIGURE 3. Schematic of the double shield aspirated thermocouple in the simplified geometry

T_{gas} is the temperature of the incoming gas sample, T_b is the temperature at the thermocouple bead and T_o is the temperature of the surroundings. This study focuses on the difference between T_b and T_{gas} . The incoming flow velocity induced by aspiration was considered. And the material properties of the cylindrical shield and the thermocouple bead were taken as stainless steel and nickel, respectively. This is not an unreasonable approximation as K-type thermocouples are composed of more than 90 % nickel.⁷

TABLE 1. Properties of solid materials

Material	Density (kg/m ³)	Specific heat (J/kg·K)	Thermal conductivity (W/m·K)
Nickel	8900	460	91.7
SS	8030	502	16.3

Radiative heat transfer was computed using a surface to surface radiation model in which the energy exchange between the two surfaces depends on the view factor, which is a geometric function involving the size, distance, and orientation of surfaces. The surfaces were taken as gray and diffuse, and taken to have a constant emissivity (ϵ) equal to 0.8 for comparison with the previous study by Blevins et al.⁵. The gas temperature (T_{gas}) was taken as constant inside and outside of the probe. An external flow velocity (U_{gas}) of 1 m/s and bead diameter of 1 mm was considered for all cases. The representative thermocouples temperature (T_b) was calculated by using a volume weighted average as follows:

$$T_b = \frac{1}{V_b} \int T \cdot dv = \frac{1}{V_b} \sum_{i=1}^N T_{b,i} \cdot dV_i \quad [1]$$

where, V_b is the total volume of the thermocouple bead, $T_{b,i}$ is the individual cell temperature and dV_i represents each cell volume for the solid bead. At the solid – fluid interface, the heat transfer coefficient for laminar flow was computed using Fourier's law:

$$q'' = k_f \left(\frac{\partial T}{\partial n} \right)_{wall} \quad [2]$$

where q'' is the heat flux to a fluid cell from a wall boundary, k_f is the thermal conductivity of the fluid and n is the local coordinate normal to the wall. For turbulent flows, FLUENT uses the law-of-the-wall for temperature derived using the analogy between heat and momentum transfer as suggested by Launder et al.⁸. The implicit solver was used to capture the transient characteristics of the heat transfer process between the fluid and the thermocouple bead.

RESULTS

Flow Field for a Realistic Double Shield Aspirated Thermocouple Geometry

Fig. 4 shows the calculated velocity field for the double shield aspirated thermocouple with an aspiration flow rate of 24 L/min. The entrance area of the inner shield is larger than its exit area, which is comprised of eight holes (see Fig. 2). This blockage effect creates a high stagnation pressure at the end of the inner shield, leading to an adverse pressure gradient inside of the inner shield. This high static pressure inside of the inner shield causes the aspirated gas flow to pass through the outer passage with a relatively high velocity. The flow blockage effect in the inner shield leads to a velocity difference between the inner and outer annular passages, which affects the convective heat transfer in the double shield aspirated thermocouple.

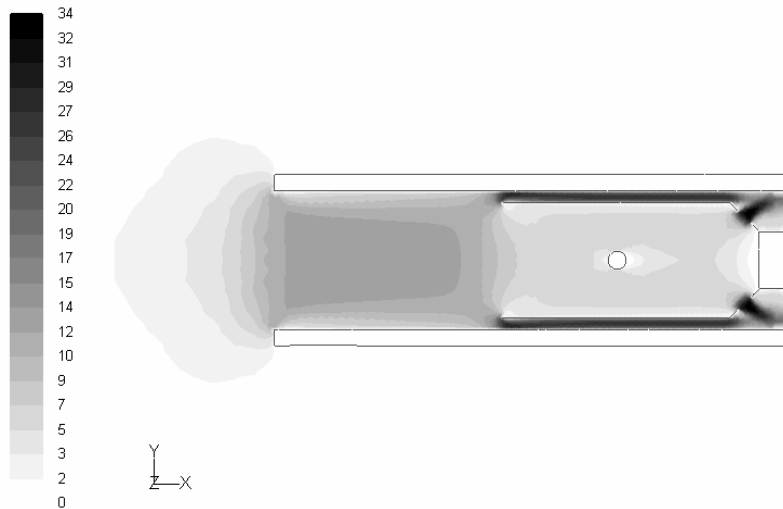


FIGURE 4. Calculated velocity field in the double shield aspirated thermocouple at the gas temperature of 300 K (aspiration flow rate = 24 L/min)

Fig. 5 presents the maximum flow velocities in the inner shield ($U_{i,max}$) and in the outer annular passage ($U_{o,max}$). The ratio of these velocities is also shown. Here, the maximum velocity ratio (ζ) is defined as:

$$\zeta = \frac{U_{o,max}}{U_{i,max}} \quad [3]$$

Fig. 5 shows that the velocity ratio increases as the aspiration flow rate increases and that the maximum velocity in the outer passage is about 3 times higher than that of the inner shield for nominal operating conditions (24 L/min at STP). This information was used to determine the velocity boundary conditions in the simplified geometry CFD heat transfer calculations and in the analytic energy balance model.

Conjugate Heat Transfer in the Simplified 3D Geometry

Fig. 6 compares the predicted temperature of the bare bead thermocouple using the algebraic simple energy balance model with the results from the CFD model considering conjugate heat transfer for an external flow with a velocity of 1 m/s and a gas temperature of 300 K and 900 K. The maximum difference of the predicted thermocouple temperature between the algebraic model and the CFD model was about 50 K for the both gas temperatures considered.

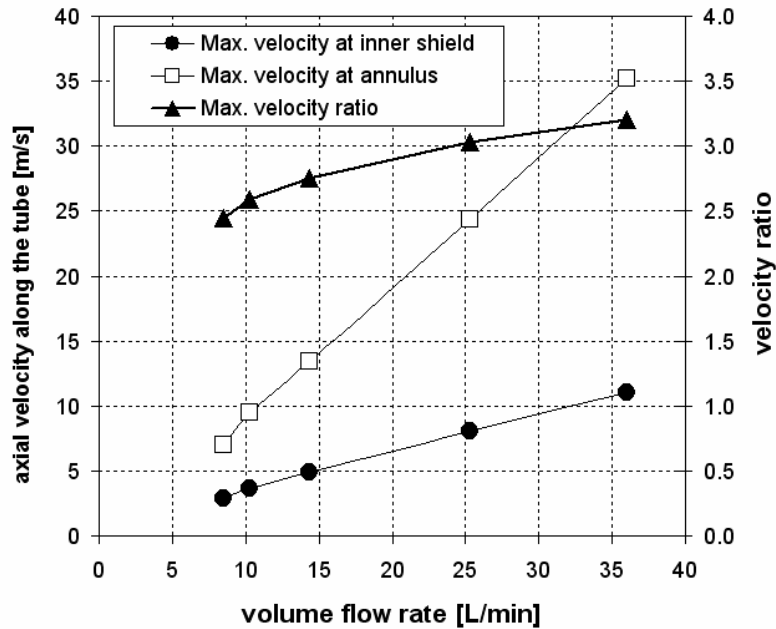


FIGURE 5. Comparison of the maximum axial velocity for a double shielded aspirated thermocouple ($T_{gas} = 300\text{ K}$)

Despite the simplicity of the algebraic model, the results predicted by the algebraic model were in reasonable agreement with the CFD model for the bare bead thermocouple exposed to the surroundings over a broad temperature range. For a 900 K gas temperature, the maximum difference between the CFD model and the algebraic model occurred for a surrounding temperature (T_o) of 300 K. The thermocouple error, that is the difference between the incoming gas temperature and the predicted thermocouple temperature, was about 160 K for the CFD model, which was 50 K higher than that of the algebraic model. But for a 300 K gas temperature, the maximum difference between CFD model and algebraic models occurred for the highest surrounding temperature, and increased with increasing surrounding temperatures. The results show that for a gas temperature of 300 K, the thermocouple error of a bare bead thermocouple exceeds 100 K, when the surrounding temperature was higher than 700 K.

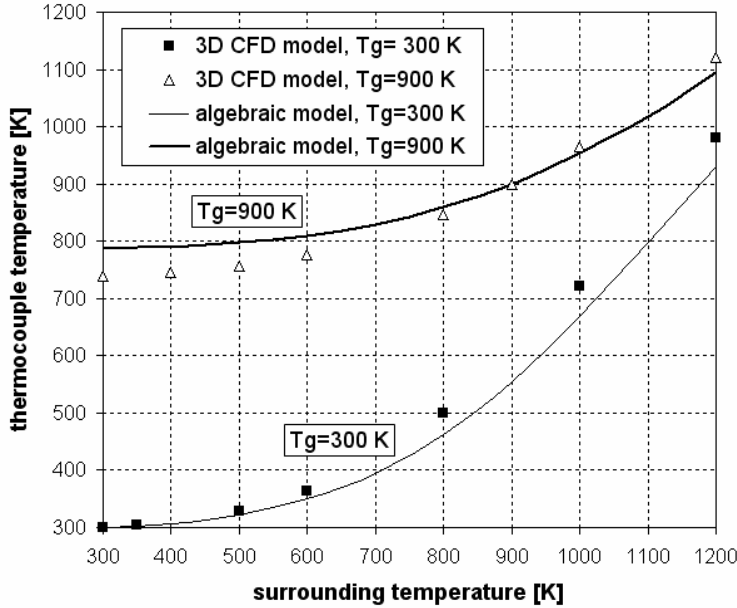


FIGURE 6. Comparisons of the predicted thermocouple temperature using the algebraic model and the 3D CFD model for the bare bead thermocouple with an external gas velocity of 1 m/s

Fig. 7 shows the thermocouple temperature of a double shield aspirated thermocouple predicted by the algebraic and CFD models for an aspiration flow rate of 24 *lpm*. The inlet boundary conditions for the aspirated gas at the inner and outer annular tubes were applied with the velocity calculated using the 3D CFD model with a realistic geometry. For a gas temperature of 600 K, both predictions are match within 1 % for the overall surrounding temperature. For gas temperature higher than 600 K, the thermocouple error predicted by the algebraic model was less than the CFD model, with the maximum difference between the algebraic model and the CFD model equal to about 50 K. But for a gas temperature of 300 K, the thermocouple error of the algebraic model was larger than the CFD model. The thermocouple error increased as the temperature difference between the gas and surrounding increased. The thermocouple error increased for the higher surrounding temperature, while it was approximately constant for a lower surrounding temperature. Considering overall performance, solution of the algebraic model shows acceptable results compared to the 3D CFD model, despite the larger number of assumptions and idealizations. This agreement shows that the algebraic energy balance model is adequate to estimate thermocouple bias for this particular application. Fig. 8 depicts the map of the calculated thermocouple error for a double shield aspirated thermocouple as a function of the thermocouple bead (T_b) and surrounding (T_o) temperatures determined using the 3D CFD model. The map shows two regimes of significant error for the thermocouple temperature measurement. The first occurs for relatively low temperature surroundings, in which the gas temperature is systematically under-predicted, notably for higher gas temperatures. The temperature error in this regime varied with the gas temperature, but was as large as -100 K for an indicated thermocouple temperature of 1200 K. The other regime with significant error occurred for high surrounding temperatures, in which the gas temperature was over-predicted.

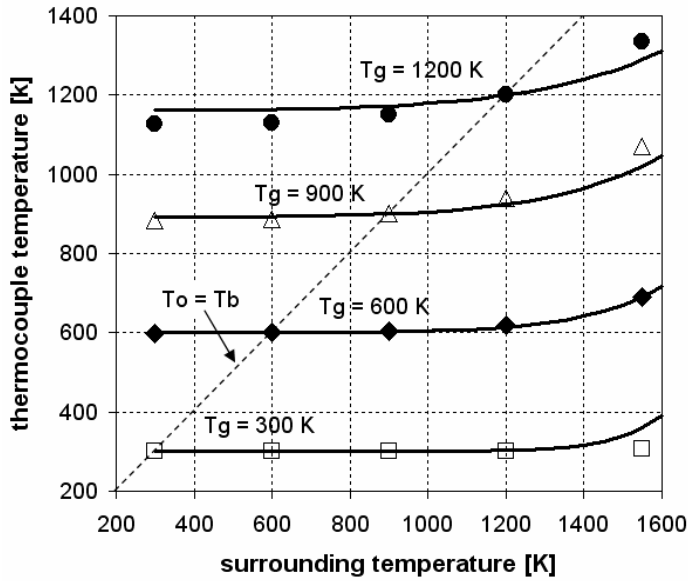


FIGURE 7. Comparison of the algebraic and CFD models of the thermocouple temperature for a double shield aspirated thermocouple with an aspiration flow of 24 lpm, where the symbols represent the CFD results and the lines represent the algebraic models).

TABLE 2. Calculated thermocouple temperature bias

T_g [K]	$T_b - T_g$ [K]			
	bare bead thermocouple		double shield aspirated thermocouple	
	$T_o = 300$ K	$T_o = 1200$ K	$T_o = 300$ K	$T_o = 1200$ K
300	0	680	0	3
900	-160	220	-10	120

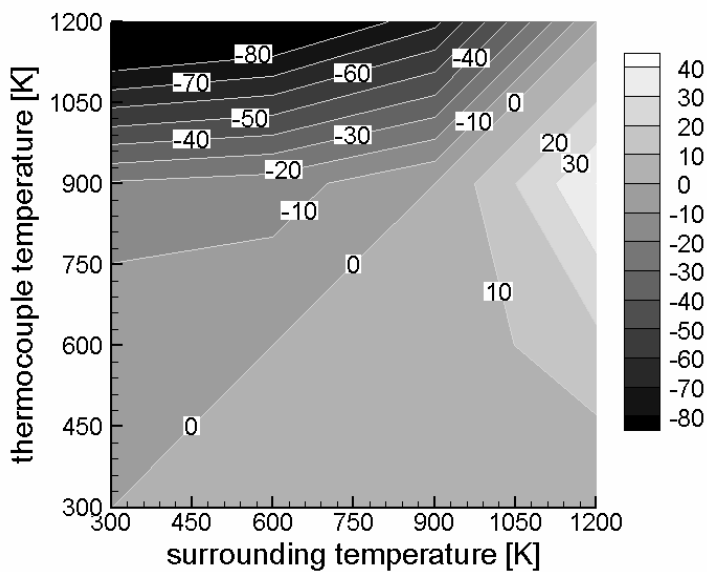


FIGURE 8. A map of the measurement bias of a double shield aspirated thermocouple as a function of the thermocouple temperature and the surrounding temperature determined using the 3D CFD model

The maximum error in this regime was as large as 40 K for a high surrounding temperature ($T_o = 1200$ K) and a thermocouple temperature of about 900 K. The results calculated by the algebraic model showed similar trends, but the magnitude of the difference was smaller. As seen in Table 2, the use of the double shield aspirated thermocouple dramatically reduced the thermocouple error as compared to a bare bead thermocouple for a gas temperature of 300 K. The temperature measured using the double shield aspirated thermocouple was close to the true gas temperature regardless of the value to the surrounding temperature (T_o). For a relatively high gas temperature (900 K), the bias of the double shield aspirated thermocouple was relatively large compared to its performance for a gas temperature of 300 K. Its performance, however, was still superior to that of the bare bead thermocouple. In summary, the use of a double shield aspirated thermocouple can be expected to reduce measurement error, particularly for lower layer compartment fire environments.

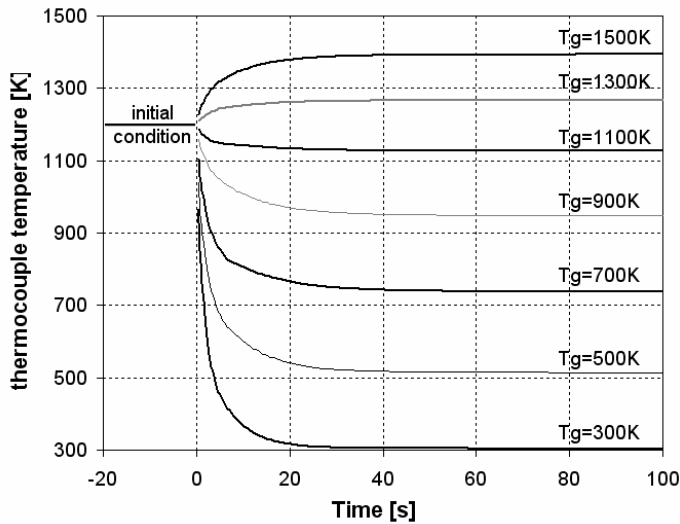


FIGURE 9. The calculated time history of the temperature of a double shielded aspirated thermocouple for various incoming gas temperatures (T_g), for a surrounding temperature of 1200 K and an aspiration flow of 24 L/min.

The time response of the thermocouple measurements was investigated using CFD modeling. The algebraic model can not provide this type of information, because the transient term in the energy balance equation is not considered. Fig. 9 shows the time history of the calculated thermocouple response for a double shield aspirated thermocouple. Initially, the gas and thermocouple temperature was assumed to be the same as the surrounding temperature and the aspiration rate was assumed to be 24 *lpm*. In the calculation, the temperature was specified to rise or fall towards the final temperature over tens of seconds, the exact time depended on the magnitude of the temperature change. In order to examine the response time for a range of initial and surrounding temperatures, a parametric study was performed. Fig. 10 compares the calculated time to reach quasi-steady state temperature as a function of the incoming gas temperature for surrounding temperature of 300 K, 600K, and 1200 K. Steady state was defined as the time when the thermocouple temperature variation was less than 1 K/s. The results showed that the thermocouple response time decreased as temperature difference between the gas and the surrounding decreased. The time to steady state varied with the incoming gas temperature, but was largest for a large incoming gas temperature. For example, for the case of a surrounding temperature of 300 K, the time to steady state took a maximum of about 50 s for an incoming gas temperature of 1200 K. The results show that the double shield aspirated thermocouple required at least 1 min to reach quasi-steady state gas temperature from the time aspiration is initiated.

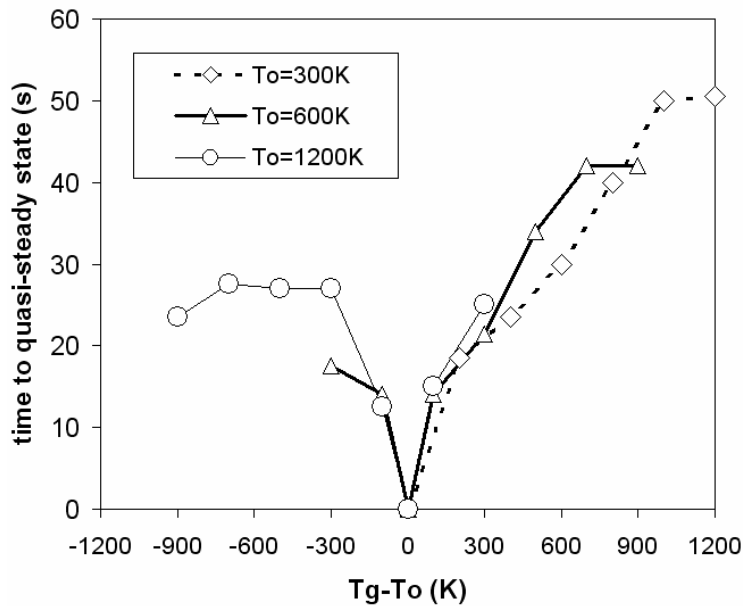


FIGURE 10. Comparison of calculated time to reach steady state as a function of the incoming gas temperature for surrounding temperatures of 300 K, 600 K, and 1200 K

CONCLUSIONS

The present study investigated the flow and heat transfer characteristics of a bare bead and a double shield aspirated thermocouple using an algebraic energy balance model and a 3D CFD model. Despite the application of additional assumptions and idealizations, calculations using the previously developed algebraic energy balance model⁵ generally showed good agreement with the results of the 3D CFD model. The algebraic model can be useful, particularly in parametric studies used to evaluate thermocouple measurement error. Consistent with previous findings, calculations show that use of the double shield aspirated thermocouple can greatly reduce the thermocouple error especially for low gas temperatures. The results, however, can still be biased by hundreds of degrees, depending on the conditions. A map of the thermocouple uncertainty for the double shield aspirated thermocouple provides information on the order of magnitude of the measurement error for a given surrounding temperature. The results of the CFD model allow determination of the transient response of the double shield aspirated thermocouple, which is helpful in the interpretation of measurement results and possibly for design of the experiment itself.

REFERENCES

1. Luo, M, "Effects of Radiation on Temperature Measurement in a Fire Environment", *Journal of Fire Science*, 15:6, 443-461, 1997.
2. Hamins, A., Maranghides, A., Mcgrattan, K.B., Ohlemiller, T.J. and Anleitner, R.L., "Experiments and Modeling of Multiple Workstations Buring in a Compartment", NIST NCSTAR 1-5E, Federal Building and Fire Safety Investigation of the World Trade Center Disaster, 2005.
3. Newman, J.S. and Croce, P.A. "A Simple Aspirated Thermocouple for Use in Fire", *Journal of Fire and Flammability*, 10:4, 327-336. 1979.
4. Brohez, S., Delvosalle, C. and Marlair, G., "A Two-thermocouples Probe for Radiation Corrections of Measured Temperatures in Compartment Fires", *Fire Safety Journal*, 39:5, 399-411, 2004.

5. Blevins, L.G. and Pitts W.M., "Modeling of Bare and Aspirated Thermocouples in Compartment Fires", Fire Safety Journal, 33: 4, 239-259, 1999.
6. Glawe, G.E., Simmons, F.S. and Stickney, T.M., "Radiation and Recovery Corrections and Time Constants of Several Chromel-Alumel Thermocouple Probe in High Temperature, High Velocity Gas Streams", NACA TN3766, 1953.
7. Fluent Inc., Fluent 6.0 User's Manual, Fluent Inc.
8. Burns, G.W. and Scroger, M.G., "The Calibration of Thermocouples and Thermocouple Materials", NIST Special Publication, 250-25, 1989.
9. Launder, B.E. and Spalding, D.B., "The Numerical Computation of Turbulent Flows," Computer Methods in Applied Mechanics and Engineering, 3:269-289, 1974.